ISSN: 2688-8645

An Extended Model for Short Wavelength Peristaltic Flow

Ding Yuan *

School of Mechanical and Electrical Engineering, Guangzhou Railway Polytechnic, Guangzhou, 511300, China

Abstract

Peristaltic flow theory is often based on the long wavelength assumption, which can be approximated by small wave number cases. This paper presents a unique approach to analyze the peristaltic flow for both short and long wavelength domains. The governing equation considering wave number is solved by combining eigen function expansion and generalized inversion methods, which is first proposed to solve peristaltic flow problems. In particular, the modified Navier-Stokes equations, considers the effects of the Trouton's elongational viscosity. The result indicates that this computational method efficiently reduces the dimensions and condition number of the matrix. The sketch of stream function shows that a trapped bolus also occurs in short wave peristaltic flow. The validity of this computational approach is demonstrated by comparing these results with existing theories.

Keywords

Short Wavelength Peristalsis; Eigen Function Expansion; Generalized Inversion Method.

1. Introduction

Peristaltic pumping, as a means of fluids transport, has a wide range of applications such as pumping corrosive fluids, foods and physiological fluids [1–5]. The problem of peristaltic pumping is very complex and difficult, due to moving walls propelling an enclosed fluid, usually a non-Newtonian fluid. Much progress has been made during the past few decades in understanding the flow mechanism of peristalsis. Most of the fluid mechanics models are mainly established on the long wavelength assumption of periodic wave peristalsis. Latham [2] was probably the first to investigate the mechanism of peristalsis in relation to mechanical pumping. Jaffrin and Shapiro [3] studied the peristaltic pumping model of plane two dimensional and with long wavelengths at low Reynolds number. Böhme et al. [4] have indicated that the flow rate is independent of viscosity when not taking into account slippage effects. It was found that the velocity field and the nonlinear pumping characteristics were influenced by the Deborah number, but not by the Weissenberg number within lubrication approximation.

Peristaltic flow in different wave shape tubes/ducts has been studied [5–8]. Srivastava et al. [5] modeled the peristaltic flow in the vas deferens by assuming it to be a non-uniform diverging channel and a tube. Hariharan [6] employed Fourier series to investigate a more realistic peristaltic transport model by evaluating non-Newtonian fluid (power law and Bingham fluid) flow in a non-uniform tube with different wall wave forms. Ellahi et al. [7] analyzed the mass and heat transfer effects on peristaltic motion in a non-uniform rectangular duct with constant viscosity and obtained the closed form solutions.

Peristaltic flow with magnetic effects has also attracted the attention of mathematicians, biomedical engineers and physicists [9–11]. Bhatti et al. [9] used the long wavelength approximation investigating the effect of magnetic field on the peristaltic transport of Carreau fluid in a three-dimensional tube. Mekheimer et al. [10] also investigated a three-dimensional peristaltic problem with the impact of lateral walls in an asymmetric rectangular duct.

ISSN: 2688-8645

In recent years, the mechanism of nanofluids induced by peristaltic wave has attracted many investigators [12–15]. Rahman [12] examined the effects of nanoparticles on the blood flow of Jeffrey fluid and taken slip effects into account. Hayat [13] and Mustafa [14] solved the peristaltic flow problem of nanofluids combining effects of Brownian motion and thermophoretic diffusion of nanoparticles. Akbar and Nadeem [15] presented the homotopy perturbation method to discuss the influence of nanofluids on the peristaltic flow of an incompressible coupled stress fluid in a two-dimensional uniform tube.

Table 1. Nomenclature

t	time
v_x, v_y	components of velocity
p	pressure
c	wave speed
a	wave amplitude
T	period
x, y	coordinate axis
Re	Reynolds number
Q	volume flow rate
$\mathbf{A}$	coefficient matrix
$\mathbf{b}$	constant matrix
$\mathbf{A}_1$, $\mathbf{A}_2$, $\mathbf{b}_1$	submatrix
$\boldsymbol{x}$, $\mathbf{C}$, $\mathbf{d}$	unknown matrix
Greek symbol	
$\boldsymbol{\tau}$	stress tensor
$\dot{\boldsymbol{\gamma}}$	strain rate tensor
λ	wavelength
λ_{jn}	characteristic root
μ_e	elongational viscosity
μ	shear viscosity
Θ	dimensionless flow rate
ψ	stream function
δ	wave number
ε	clearance
ξ	solution vector
η	elongation index
η_m	average η in a period
φ	amplitude ratio
ω	angular speed

For the peristaltic flow models, the constitutive relationships of materials have been enriched from the simplest Newton fluid to various complex non-Newtonian fluids. In addition, different wave shapes, temperature or nanofluid effects have also been taken into account. Available studies have demonstrated that if the wavelength is much larger than the amplitude, predictions given by long wavelength assumption are sufficiently accurate. However, it is well known that the long wavelength assumption breaks down when the wave number is not small. To overcome such deficiencies, several peristaltic flow theories were developed. Higdon [16] presented a boundary-integral method, solving the integral governing equations of Stokes flow in arbitrary two-dimensional domains. Burns and Parkes [17] indicated that for small aspect

ISSN: 2688-8645

ratios, the waveform could be approximated by a Fourier series, but more coefficients were needed, and the method required the aid of a digital computer.

Inspired by the application of short wavelength peristaltic flow, the goal of present study is to determine the peristaltic flow of short wavelength with a closed cavity. The constitutive equations of the presented model consider Trouton elongational viscosity to approximate inelastic polymeric materials' constitutive relationship. Through applying eigen function expansion method to express the periodic function of streamlines, the governing equations are fully solved by the generalized inversion method. The series solutions are computed and then examined with the help of graphs of streamlines and flow rates.

2. Theory

2.1. The Modified Navier-Stokes Equations

According to the hydromechanics theory, incompressible Stokes flow in the absence of body forces and at zero Reynolds number are determined by Eqs. (1)–(3):

$$\frac{\partial v_x}{\partial x}+\frac{\partial v_y}{\partial y}=0 \tag{1}$$

$$\frac{\partial p}{\partial x}=\frac{\partial \tau_{xx}}{\partial x}+\frac{\partial \tau_{xy}}{\partial y} \tag{2}$$

$$\frac{\partial p}{\partial y}=\frac{\partial \tau_{xy}}{\partial x}+\frac{\partial \tau_{yy}}{\partial y} \tag{3}$$

where p is the pressure, v_x and v_y are the respective velocity components in the axial and transverse directions, $\tau_{ij}=\mu\dot{\gamma}_{ij}$ is the partial stress and defined as:

$$\tau_{xx}=\mu\dot{\gamma}_{xx} \tag{4}$$

$$\tau_{xy}=\mu\dot{\gamma}_{xy} \tag{5}$$

$$\tau_{yy}=\mu\dot{\gamma}_{yy} \tag{6}$$

in which μ is the shear viscosity, $\dot{\gamma}_{ij}=\left(\frac{\partial v_i}{\partial x_j}+\frac{\partial v_j}{\partial x_i}\right)$ is the rate of strain tensor.

In the field of polymer processing, polymeric materials are usually non-Newtonian fluids, whose constitutive relationships are different from Newtonian fluids. As changes in the partial stresses are induced by changes of the viscosity, here, Eqs. (5) and (6) are modified to suit for inelastic polymeric materials which satisfies the Trouton law. The Trouton law indicates that the elongational viscosity of Newtonian fluids and inelastic polymer can usually be approximated as 3 times the shear viscosity at low shearing rates [18,19]. Here, effects of the Trouton law' elongational viscosity are considered by modifying the elongational viscosity in Eqs. (5) and (6) through an approximation, assuming that elongational viscosity is equal to 3 times the shear viscosity,

$$\mu_e=3\mu \tag{7}$$

Replacing Eq. (7) into Eqs. (5) and (6) respectively, the partial stresses are modified as follows:

$$\tau_{xx}=3\mu\dot{\gamma}_{xx} \tag{8}$$

$$\tau_{yy}=3\mu\dot{\gamma}_{yy} \tag{9}$$

Substituting the Eqs. (8) and (9) into Eqs. (5) and (6) respectively, and using Eq. (1), the two-dimensional momentum conservation equations are modified to be

ISSN: 2688-8645

$$\frac{\partial p}{\partial y} = 5\mu \frac{\partial^2 v_y}{\partial y^2} + \mu \frac{\partial^2 v_y}{\partial x^2}$$
$$\frac{\partial p}{\partial x} = 5\mu \frac{\partial^2 v_x}{\partial x^2} + \mu \frac{\partial^2 v_x}{\partial y^2} \quad (10)$$

Now introducing streamline function ψ,

$$v_x = \frac{\partial \psi}{\partial y}, v_y = -\frac{\partial \psi}{\partial x},$$

Replacing $v_x = \frac{\partial \psi}{\partial y}$ and $v_y = -\frac{\partial \psi}{\partial x}$ into Eq. (10) and noticing that $\frac{\partial}{\partial x}\frac{\partial p}{\partial y} = \frac{\partial}{\partial y}\frac{\partial p}{\partial x}$ yields the following equation

$$\frac{\partial^4 \psi}{\partial z^4} + 10\frac{\partial^4 \psi}{\partial y^2 \partial z^2} + \frac{\partial^4 \psi}{\partial y^4} = 0 \quad (11)$$

Eq. (11) is the governing equation considering the Trouton law and is applied for peristaltic flow analysis of short wavelength structures.

2.2. Statement of Peristaltic Flow

The peristaltic boundary *h* is defined by the following equation:

$$h = a(1 - \cos 2\pi \frac{x - ct}{\lambda}) + \varepsilon \quad (12)$$

Eq. (12) shows that a progressive wave of amplitude *a*, wavelength λ, clearance ε and velocity *c* passes along the tube in the positive *x*-direction. The velocity components in the *x* and *y* directions are v_x and v_y, respectively (see Fig. 1).

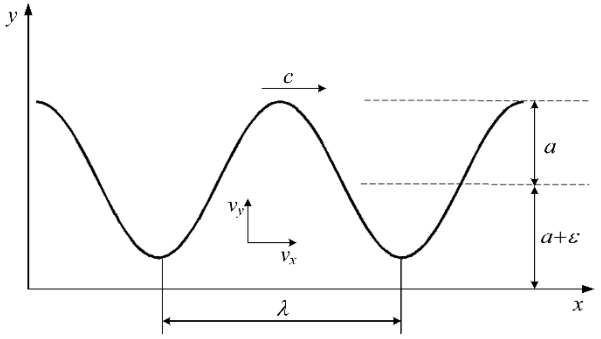

Fig 1. Schematic diagram of the physical model

Applying the governing Eq. (11), the following non-dimensional quantities are introduced:

$$\bar{x} = \frac{x}{\lambda}, \bar{y} = \frac{y}{a}, \bar{u} = \frac{v_x}{c}, \bar{v} = \frac{v_y}{c\delta}, \delta = \frac{a}{\lambda}, \bar{P} = \frac{a^2 P}{\mu c \lambda}, \mathrm{Re} = \frac{\rho c a}{\mu} \quad (13)$$

where *Re* is the Reynolds number and δ is the dimensionless wave number. In terms of these non-dimensional variables, the equations of continuity and momentum conservation can be expressed in non-dimensional form:

From Eq. (14), it is observed that the terms containing δ will be eliminated because compared to the leading term, terms with δ are small quantity if the long wavelength approximation is used. Here, the goal is to solve the full Eq. (14) under a complex moving boundary condition with an enclosed fluid.

ISSN: 2688-8645

$$\delta\frac{\partial\overline{v_x}}{\partial\overline{x}}+\frac{\partial\overline{v_y}}{\partial\overline{y}}=0$$
$$\frac{\partial\overline{p}}{\partial\overline{y}}=5\delta^3\frac{\partial^2\overline{v_y}}{\partial\overline{y}^2}+\delta\frac{\partial^2\overline{v_y}}{\partial\overline{x}^2} \tag{14}$$
$$\frac{\partial\overline{p}}{\partial\overline{x}}=5\delta^2\frac{\partial^2\overline{v_x}}{\partial\overline{x}^2}+\frac{\partial^2\overline{v_x}}{\partial\overline{y}^2}$$

2.3. Mathematical Model and Solution

As the governing Eq. (11) is a linear partial differential equation, it is easy to obtain the general solution but it is difficult to acquire the specific solution for this moving nonlinear boundary. As the boundary varies periodically with *x,* it follows that ψ is also a periodic function of *x* with wavelength λ. Therefore, we apply the eigen function expansion method and assume the function $\psi(x, y)$ as Fourier cosine series in the form:

$$\psi=\sum_{n=1}^{N}f_n(y)\cos\left(n\pi\frac{x\text{-}ct}{\lambda}\right) \tag{15}$$

Substituting Eq. (15) into Eq. (11), yields the following equation

$$f_n^{(4)}(y)\text{-}10\left(\frac{n\pi}{\lambda}\right)^2 f_n^{(2)}(y)+\left(\frac{n\pi}{\lambda}\right)^4 f_n(y)=0 \tag{16}$$

The solutions to Eq. (16) is

$$f_n(y)=C_{1n}e^{\lambda_{1n}y}+C_{2n}e^{\lambda_{2n}y}+C_{3n}e^{\lambda_{3n}y}+C_{4n}e^{\lambda_{4n}y} \tag{17}$$

where the characteristic roots of Eq. (16) are as follows:

$\lambda_{1n}=\sqrt{5+\sqrt{24}}\,\frac{n\pi}{\lambda},\lambda_{2n}=-\sqrt{5+\sqrt{24}}\,\frac{n\pi}{\lambda},\lambda_{3n}=\sqrt{5-\sqrt{24}}\,\frac{n\pi}{\lambda},\lambda_{4n}=-\sqrt{5-\sqrt{24}}\,\frac{n\pi}{\lambda},$ Thus, we have the general solution of the stream function:

$$\begin{aligned}\psi&=\sum_{n=1}^{N}f_n(y)\cos\left(n\pi\frac{x\text{-}ct}{\lambda}\right)\\&=\sum_{n=1}^{N}(C_{1n}e^{\lambda_{1n}y}+C_{2n}e^{\lambda_{2n}y}+C_{3n}e^{\lambda_{3n}y}+C_{4n}e^{\lambda_{4n}y})\cos\left(n\pi\frac{x\text{-}ct}{\lambda}\right)\\&=\sum_{n=1}^{N}\sum_{i=1}^{4}C_{jn}e^{\lambda_{jn}y}\cos\left(n\pi\frac{x\text{-}ct}{\lambda}\right)\end{aligned} \tag{18}$$

where the coefficients in Eq. (18) are to be found in terms of velocity *c,* wavelength λ and characteristic roots from the boundary conditions:

$$v_x(x,h,t)=0,\ v_x(x,0,t)=0,v_y(x,h,t)=e\omega\sin(2\pi\frac{x-ct}{\lambda}),v_y(x,0,t)=0 \tag{19}$$

where *h* is the upper peristaltic boundary, with $h=a(1-\cos 2\pi\frac{x-ct}{\lambda})+\varepsilon$. With the available solutions of the stream function ψ, the v_x and v_y are determined.

$$v_x=\sum_{n=1}^{N}\sum_{j=1}^{4}C_{jn}\lambda_{jn}e^{\lambda_{jn}y}\cos\left(n\pi\frac{x\text{-}ct}{\lambda}\right) \tag{20}$$

$$v_y=\sum_{n=1}^{N}\sum_{j=1}^{4}C_{jn}e^{\lambda_{jn}y}\frac{n\pi}{\lambda}\sin\left(n\pi\frac{x\text{-}ct}{\lambda}\right) \tag{21}$$

ISSN: 2688-8645

Introduce Eqs. (20) and (21) into Eq. (19), we have the following equations:

$$\begin{aligned}
&\sum_{n=1}^{N}\sum_{j=1}^{4} C_{jn}\lambda_{jn}e^{\lambda_{jn}h(x)}\cos\left(n\pi\frac{x\text{-}ct}{\lambda}\right)=0\\
&\sum_{\mathrm{n}=1}^{N}\sum_{j=1}^{4} C_{jn}e^{\lambda_{jn}h(x)}\frac{n\pi}{h}\sin\left(n\pi\frac{x\text{-}ct}{\lambda}\right)=\frac{a}{2}\omega\sin\left(2\pi\frac{x\text{-}ct}{\lambda}\right)\\
&\sum_{n=1}^{N}\sum_{j=1}^{4} C_{jn}\lambda_{jn}\cos\left(n\pi\frac{x\text{-}ct}{\lambda}\right)=0\\
&\sum_{n=1}^{N}\sum_{j=1}^{4} C_{jn}\sin\left(n\pi\frac{x\text{-}ct}{\lambda}\right)=0
\end{aligned} \tag{22}$$

As the upper boundary y is a function of x, not coinciding with a constant value, the standard boundary value problem technique is not an acceptable method for evaluating the constants in the series for the stream function ψ. The idea of the technique used here is to discrete the upper boundary h into several points and make as many the points as possible meet boundary conditions, because the accuracy of the solution depends on the number of points. First, the lower boundary is truncated into K points, and correspondingly, the upper boundary is also truncated into K points . The included constants are evaluated by satisfying boundary conditions at a selected number of points along a wavelength.

It can be seen that Eq. (22) contain $4N$ unknowns (C_{1n}, C_{2n}, C_{3n}, C_{4n}, n=1, 2, 3… N), with N the number of expansion terms of streamline function ψ. One boundary point establishes 2 equations according to v_x and v_y. The total number of boundary points is $2K$, such that the total number of equations is $4K$. If the expansion number N of ψ is equal to the number of lower boundary points K, then Eq. (22) could be solved directly. Otherwise, if N is less than K, the number of equations is more than the unknowns, leading Eq. (22) overdetermined, and usually there is no solution, while the problem will be solvable in terms of generalized inversion method. The essence to solve Eq. (22) using the generalized inversion method is to find the solution satisfying the minimum requirement of $\|\mathbf{Ax}-\mathbf{b}\|_2$ (where $\mathbf{A}$ and $\mathbf{b}$ are the coefficient and constant matrixes of Eq. (22), respectively, $\mathbf{x}$ is the unknown matrix of Eq. (22). Both of the above-mentioned approaches have been addressed and the results indicate that the generalized inversion approach provides better performance because it avoids overly large condition numbers caused by a large sparse matrix with the increasing boundary points.

Here, we discuss the process of using the generalized inversion method for Eq. (22). Eq. (22) can be simplified into Eqs. (23)–(26) respectively.

$$\sum_{n=1}^{N}\sum_{j=1}^{4} C_{jn}\lambda_{jn}e^{\lambda_{jn}h(x_i)}\cos\left(n\pi\frac{x_i\text{-}ct}{\lambda}\right)=0,\quad (i=1\ldots K) \tag{23}$$

$$\sum_{\mathrm{n}=1}^{N}\sum_{j=1}^{4} C_{jn}e^{\lambda_{jn}h(x_i)}\frac{n\pi}{h}\sin\left(n\pi\frac{x_i\text{-}ct}{\lambda}\right)=\frac{a}{2}\omega\sin\left(2\pi\frac{x_i\text{-}ct}{\lambda}\right),\quad (i=1\ldots K) \tag{24}$$

$$\sum_{j=1}^{4} C_{jn}\lambda_{jn}=0,\quad (n=1\ldots N) \tag{25}$$

$$\sum_{j=1}^{4} C_{jn}=0,\quad (n=1\ldots N) \tag{26}$$

We rewrite the Eqs. (23)–(26) into partitioned matrix forms as follows:

$$\begin{pmatrix}\mathbf{A}_1\\ \cdots\\ \mathbf{A}_2\end{pmatrix}\mathbf{C}=\begin{pmatrix}\mathbf{b}_1\\ \cdots\\ \mathbf{0}\end{pmatrix} \tag{27}$$

ISSN: 2688-8645

where $\mathbf{A}_1$ and $\mathbf{b}_1$ are the coefficient and constant matrixes of Eqs. (23)–(24), $\mathbf{A}_2$ is the coefficient matrix of Eqs. (17.3)–(17.4). $\mathbf{C}$ is the unknown matrix of Eqs. (23)–(26), with $\mathbf{C}=(C_{11},C_{21},C_{31},C_{41}\ldots C_{1N},C_{2N},C_{3N},C_{4N})^{\mathrm{T}}$.

The equation number of Eqs. (23)–(26) is $2K+2N$, and the number of unknowns is $4N$. Note that the second of Eq. (27), $\mathbf{A}_2\mathbf{C}=0$, is a set of homogeneous linear equations and $\mathbf{A}_2$ irrelevant to x, so we first solve $\mathbf{A}_2\mathbf{C}=0$, and the basic solution is obtained:

$$\mathbf{C}=d_1\boldsymbol{\xi}_1+d_2\boldsymbol{\xi}_{2+\ldots+}\, d_{2N}\boldsymbol{\xi}_{2N} \tag{28}$$

where($\boldsymbol{\xi}_1, \boldsymbol{\xi}_2,\ldots\boldsymbol{\xi}_{2N}$) are the solution vectors of $\mathbf{C}$ (the size of vector $\mathbf{C}$ is $4N\times 2N$, and $d_1, d_2,\ldots, d_{2N}$ are the unknown constants that are determined by substituting Eq. (28) into Eq. (29):

$$\mathbf{A}_{1\,(2k\times 4N)}\,\mathbf{C}_{\,(4N\times 1)}=\boldsymbol{b}_{1\,(2k\times 1)} \tag{29}$$

The equation number of Eq. (29) is $2K$, if $N=K$, Eq. (29) can be solved directly. However, in order to improve the accuracy, K is usually far greater than N (e.g., K=130, N=2). As the undetermined coefficients are d_1, d_2 … d_{2N}, Eq. (29) should be written as

$$\mathbf{A}'_{1\,(2K\times 2N)}\mathbf{d}_{(2N\times 1)}=\mathbf{b}_{1(2K\times 1)} \tag{30}$$

where $\mathbf{A}'_{1\,(2K\times 2N)}=\mathbf{A}_{1(2K\times 4N)}(\xi_1,\xi_2,\ldots,\xi_{2N})_{(4N\times 2N)}$, $\mathbf{d}=(d_1,d_2,\ldots,d_{2N})_{(2N\times 1)}$. It is found from Eq. (30) that the dimensions of Eqs. (23)–(26) are deduced from $2N+2K$ to $2K$.

By left multiplicity $(\mathbf{A}'_1)^{\mathrm{T}}_{(2N\times 2K)}$ in Eq. (30), where $(\mathbf{A}'_1)^{\mathrm{T}}$ is the transpose matrix of $\mathbf{A}'_1$, Eq. (30) becomes

$$(\mathbf{A}'_1)^{\mathrm{T}}_{(2N\times 2K)}\mathbf{A}'_{1\,(2K\times 2N)}\mathbf{d}_{(2N\times 1)}=(\mathbf{A}'_1)^{\mathrm{T}}_{(2N\times 2K)}\mathbf{b}_{1(2K\times 1)} \tag{31}$$

Eq. (31) reveals that the dimensions of Eq. (30) is further reduced to $2N$. It can be seen that this technique finally reduces the dimensions of Eqs. (23)–(26) from $2N+2K$ to $2N$, making the solution of Eqs. (23)–(26) become feasible. $\mathbf{A}'_1$ is a full column rank matrix, the generalized inverse of Eq. (31) based on the least-square method is

$$\mathbf{A}^{-}_{1l}=\left((\mathbf{A}'_1)^{\mathrm{T}}\mathbf{A}'_1\right)^{-1}_{(2N\times 2N)}(\mathbf{A}'_1)^{\mathrm{T}}_{(2N\times 2K)} \tag{32}$$

Then, the solution of Eq. (30) is

$$\mathbf{d}_{(2N\times 1)}=\mathbf{A}^{-}_{1l(2N\times 2K)}\mathbf{b}_{1(2K\times 1)} \tag{33}$$

Substituting Eq. (33) into Eq. (28), then $\mathbf{C}$ is obtained. The relevant calculation is carried out by using MATLAB for programming. It is found that the numerical solutions are precise enough when N = 2, K = 130. With the available solution of $\mathbf{C}$, the stream function is determined. Eq. (34) gives the expression of the stream function of a case when t = 0, a = 6 mm, λ = 10 mm, δ = 0.6, c = 10 mm/s and ε=0.

$$\begin{aligned}\psi=&(-3.7574\times10^{-13}\mathrm{e}^{988.4281y}+1.9258\times10^{-9}\mathrm{e}^{988.4281y}+8.5707\times10^{-9}\mathrm{e}^{99.8515y}\\&-1.0496\times10^{-8}\mathrm{e}^{-99.8515y})\cos(100\pi x)+(7.9519\times10^{-12}\mathrm{e}^{1976.9y}-0.0238\mathrm{e}^{-1976.9y}\\&-0.1059\mathrm{e}^{199.7030y}+0.1297\times10^{-8}\mathrm{e}^{199.7030y})\cos(200\pi x)\end{aligned} \tag{34}$$

A MATLAB program is developed to solve the streamline function Ψ.

3. Graphical Results and Discussion

The validity of the technique is demonstrated by examining the behavior of the stream function and velocity. The computational domain is taken to be one wavelength and different wave lengths are presented.

ISSN: 2688-8645

3.1. Velocity Distribution

Fig. 2(a) shows a graphic of a typical flow field at t=0 time in the laboratory frame, with the a = 6 mm, λ = 10 mm, δ = 0.6, ε = 0 and c = 10 mm/s. It can be seen that a wave of contraction is passing along the channel to the right. Note that the velocity profile in the wave cross section is pointing to the right as well, consistent with wave speed spreading direction. However, in the expansion section, the velocity profile is pointing to the left, due to the conservation of volume of the incompressible fluid. The fluid sticks to the channel wall, because the viscous boundary assumption is used (see Fig. 2(a)-(b)).

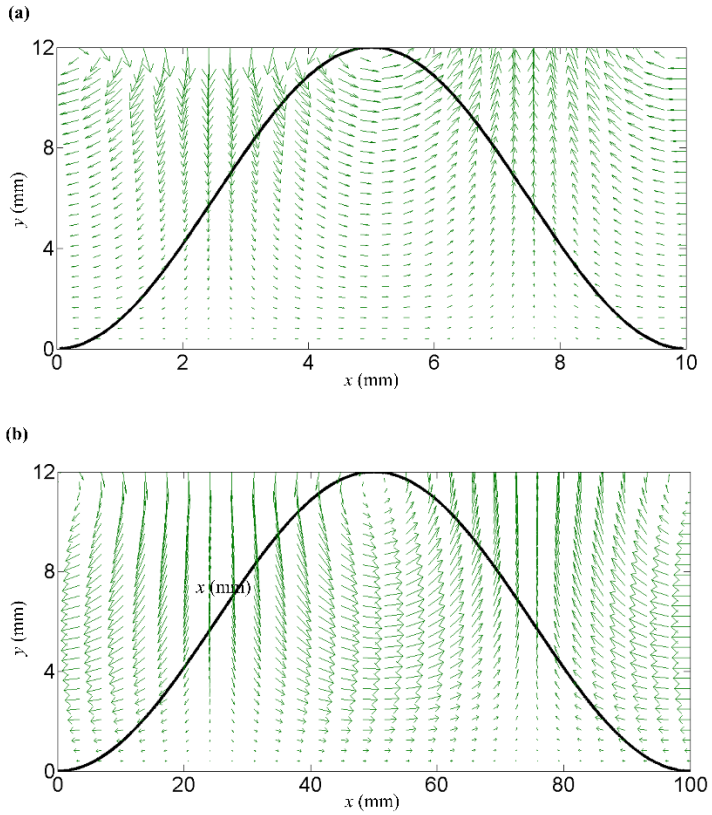

Fig 2. Velocity profiles for multiple wavelengths at a = 6 mm, c = 20 mm/s, (a) short wavelength, λ = 10 mm, δ = 0.6, (b) long wave wavelength, λ = 100 mm, δ = 0.06.

3.2. Trapping Phenomenon

Trapping is an interesting phenomenon of peristalsis, the formation and transport of an internally circulating region of fluid moving with the wave. These fluid boluses would not be evident in the laboratory frame, about which previous studies have also draw the conclusion [20, 21]. However, in a frame of reference moving at the wave speed c (the wave frame), they would appear as zones of recirculation as shown in Fig. 3(a)-(f). It has been shown in Ref. [3] that trapping is relative with the degree of geometric occlusion and occurs at a larger amplitude ratio φ

$$\phi = \frac{a}{a + \varepsilon} \tag{35}$$

Three examples of peristaltic flow were computed using the parameter values of a = 6 mm, λ = 10 mm, δ = 0.6, c = 20 mm/s with three different clearances ε = 0, 2 and 4 mm, respectively. Fig. 3(a) and Fig. 3(c) show streamlines in the laboratory frame for narrower channels where ε = 0 and 2 mm. Fig. 3(b) and (d) depict streamlines in the wave frame, and here the bolus formation are evident. Fig. 3(e) shows streamlines in the laboratory frame and Fig. 3(f) shows streamlines in the wave frame for the wider channel φ = 0.6, where trapping has not occurred.

ISSN: 2688-8645

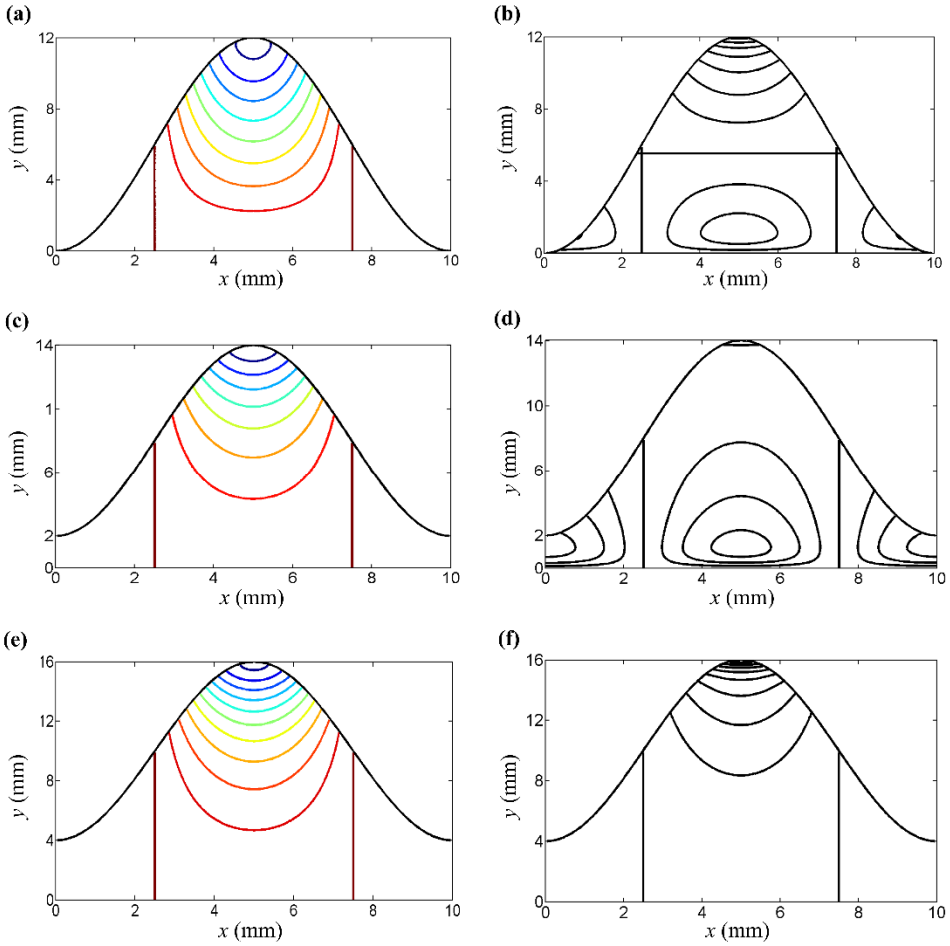

Fig 3. Streamlines of a = 6 mm, λ = 20 mm, δ = 0.3, c = 20mm/s, in (a) the laboratory frame and (b) the wave frame, φ = 1; (c) the laboratory frame and (d) the wave frame, φ = 0.75; (e) the laboratory frame and (f) the wave frame, φ = 0.6.

3.3. Pumping Characteristics

A quantity of practical interest is the mean flow rate:

$$\overline{Q} = \frac{1}{T}\int_0^T \int_0^h U dy dt \tag{36}$$

where $T = \lambda/c$, and the dimensionless mean flow is defined as follow:

$$\Theta = \frac{\overline{Q}}{ac} \tag{37}$$

We will use Eq. (37) to compare our computation with previous analytical results. Shapiro *et al.* [3] analyzed peristaltic pumping in Stokes flow with infinite wavelength. This assumption results in Poiseuille flow instantaneously at every cross section. They computed the dimensionless mean flow:

$$\frac{a^2}{\mu c \lambda}\Delta p_\lambda = \frac{3}{2}\frac{\phi^2}{\left(1-\phi^2\right)^{\frac{5}{2}}}\left[3 - \frac{2+\phi^2}{\phi}\Theta\right] \tag{38}$$

When $\Delta p_\lambda = 0$, Eq. (38) is simplified into Eq. (39)

$$\Theta = \frac{3\phi}{2+\phi^2} \tag{39}$$

ISSN: 2688-8645

Fig. 4 gives a comparison of the proposed generalized inverse method solutions from the modified Navier-Stokes equations with the previous results. It is found that the calculated results of the dimensionless mean flow are less than that given by Eq. (39) This is because Eq. (39) assumes that $\Delta p_\lambda = 0$, however, in real practice Δp_λ is usually greater than zero, which leads to the $\Theta \le \frac{3\phi}{2+\phi^2}$.

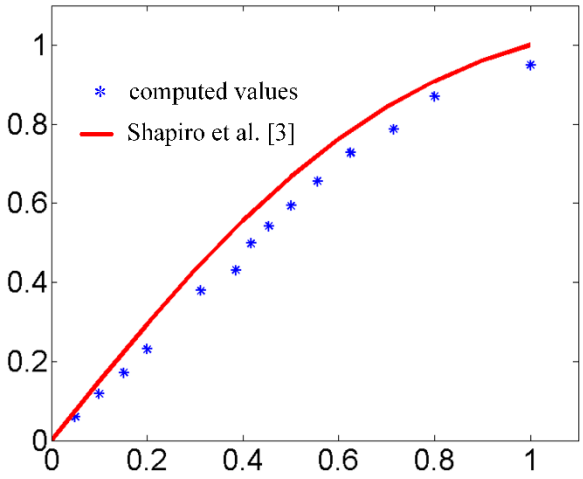

Fig 4. Dimensionless mean flow as a function of the amplitude ratio φ; a = 6 mm, λ =10 mm

4. Conclusion

In this paper, a modified governing equation considering the Trouton law is established and a computational method is presented for solving the governing equation. This technique, combing the eigen function expansion and generalized inversion methods, is first used to solve the peristaltic problem. This calculation method is found simple, efficient and has a good convergence. In future works, this model will be applied to cases of non-uniform waves and also expected to be extended to other constitutive relationships and three dimensions.

Acknowledgments

The study was supported by Guangzhou Railway Polytechnic Newly introduced talent research project (GTXYR2303).

References

[1] Z. Poursharifi, K. Sadeghy, On the use of Lattice–Boltzmann method for simulating peristaltic flow of viscoplastic fluids in a closed cavity, J. Non-Newton Fluid. 243 (2017) 1–15.

[2] T.W. Latham, Fluid Motions in Peristaltic Pump(M.S. Thesis) Massachusetts Institute of Technology, Cambridge, M.A., 1966.

[3] A.H. Shapiro, M.Y. Jaffrin, S.L. Weinberg, Peristaltic pumping with long wavelengths at low Reynolds number, J. Fluid Mech. 37(4) (1969) 799–825.

[4] G. Böhme, A. Müller, Analysis of non-Newtonian effects in peristaltic pumping, J. Non-Newton Fluid. 201 (2013) 107–119.

[5] B.B. Gupta, V. Seshadri, Peristaltic pumping in non-uniform tubes, J. BioMech. 9 (2) (1976) 105–109.

[6] P. Hariharan, V. Seshadri, R. K. Banerjee, Peristaltic transport of non-Newtonian fluid in a diverging tube with different wave forms, Math. Comput. Model. 48 (7) (2008) 998–1017.

[7] R. Ellahi, M. M. Bhatti, K. Vafai. Effects of heat and mass transfer on peristaltic flow in a non-uniform rectangular duct, Int. J. Heat Mass Transf. 71 (4) (2014) 706–719.

[8] M. Abbas, Y.Q. Bai, M.M. Bhatti, M.M. Rashidi. Three dimensional peristaltic flow of hyperbolic tangent fluid in non-uniform channel having flexible walls, Alex. Eng. J. 55 (1) (2016) 653–662.

[9] R. Ellahi, M.M. Bhatti, C.M. Khalique, Three-dimensional flow analysis of Carreau fluid model induced by peristaltic wave in the presence of magnetic field, J. Mol. Liq. 241 (2017) 1059–1068.

[10] K.S. Mekheimer, Effect of the induced magnetic field on peristaltic flow of a couple stress fluid. Phys. Lett. A. 372 (23) (2008) 4271–4278.

[11] A. Ebaid, A new numerical solution for the MHD peristaltic flow of a biofluid with variable viscosity in circular cylindrical tube via Adomian decomposition method. Phys. Lett. A. 372 (23) (2008) 5321-5328.

[12] S.U. Rahman, R. Ellahi, S. Nadeem, Q.M.Z. Zia, Simultaneous effects of nanoparticles and slip on Jeffrey fluid through tapered artery with mild stenosis, J. Mol. Liq. 218 (2016) 484–493.

[13] T. Hayat, H. Yasmin, B. Ahmad, B. Chen, Simultaneous effects of convective conditions and nanoparticles on peristaltic motion, J. Mol. Liq. 193 (2014) 74–82.

[14] M.Mustafa, S. Hina, T. Hayat, A. Alsaedi, Influence of wall properties on the peristaltic flow of a nanofluid: Analytic and numerical solutions. Int. J. Heat Mass Transf. 55 (2012) 4871–4877.

[15] S. Nadeem. N.S. Akbar, N. Bibi, S. Ashiq .Influence of heat and mass transfer on peristaltic flow of a third order fluid in a diverging tube, Commun. Nonlinear Sci. Numer. Simul. 15 (10) (2010) 2916–2931.

[16] J.J.L. Higdon. Stokes flow in arbitrary two-dimensional domains: shear flow over ridges and cavities, J. Fluid Mech. 25 (159) (1985) 195–226.

[17] J.C. Burns, T. Parkes, Peristaltic motion, J. Fluid Mech. 29 (4) (1967) 731–743.

[18] R.G Larson, Constitutive equations for polymer melts and solution, Butterworths, Boston, 1988.

[19] Taha Sochi, Non-Newtonian flow in porous media, Polymer 51 (22) (2010) 5007–5023.

[20] L.J. Fauci, Peristaltic Pumping of Solid Particles, Comput. Fluids. 21 (4) (1992) 583–598.

[21] K.K. Raju, R. Devanathan, Peristaltic motion of a non-Newtonian fluid, Rheol. Acta. 11(2) (1972) 170–178.